Biochimica et Biophysica Acta 1798 (2010) 624–636

Contents lists available at ScienceDirect

Biochimica et Biophysica Acta

journal homepage: www.elsevier.com/locate/bbamem

Selective localization of phosphatidylcholine-derived signaling in detergent-resistant membranes from synaptic endings

M.V. Mateos, G.A. Salvador *, N.M. Giusto

Instituto de Investigaciones Bioquímicas de Bahía Blanca, Universidad Nacional del Sur and Consejo Nacional de Investigaciones Científicas y Técnicas, CC 857, B8000FWB Bahía Blanca, Argentina

ARTICLE INFO

Article history:
Received 23 September 2009
Received in revised form 19 November 2009
Accepted 14 December 2009
Available online 21 December 2009

Keywords:
Detergent-resistant membrane
Synaptic ending
Aging
PC-PLC
PLD
DAG

ABSTRACT

Detergent-resistant membranes (DRMs) are a class of specialized microdomains that compartmentalize several signal transduction processes. In this work, DRMs were isolated from cerebral cortex synaptic endings (Syn) on the basis of their relative insolubility in cold Triton X-100 (1%). The lipid composition and marker protein content were analyzed in DRMs obtained from adult and aged animals. Both DRM preparations were enriched in Caveolin, Flotillin-1 and c-Src and also presented significantly higher sphingomyelin (SM) and cholesterol content than purified Syn. Total phospholipid-fatty acid composition presented an increase in 16:0 (35%), and a decrease in 20:4n-6 (67%) and 22:6n-3 (68%) content in DRM from adults when compared to entire synaptic endings. A more dramatic decrease was observed in the 20:4n-6 and 22:6n-3 content in DRMs from aged animals (80%) with respect to the results found in adults. The coexistence of phosphatidylcholine-specific-phospholipase C (PC-PLC) and phospholipase D (PLD) in Syn was previously reported. The presence of these signaling pathways was also investigated in DRMs isolated from adult and aged rats. Both PC-PLC and PLD pathways generate the lipid messenger diacylglycerol (DAG) by catalyzing PC hydrolysis. PC-PLC and PLD1 localization were increased in the DRM fraction. The increase in DAG generation (60%) in the presence of ethanol, confirmed that PC-PLC was also activated when compartmentalized in DRMs. Conversely, PLD2 was excluded from the DRM fraction. Our results show an age-related differential fatty acid composition and a selective localization of PC-derived signaling in synaptic DRMs obtained from adult and aged rats.

1. Introduction

Membrane rafts are small (10–200 nm), heterogeneous, sterol- and sphingolipid-enriched domains. Although enrichment in cholesterol (Chol) and sphingolipids is the main characteristic of membrane rafts, they also contain specific subpopulations of membrane proteins often being enriched in glycophosphoinositol-linked proteins (GPI-proteins), specific tyrosine kinases, heterotrimeric G-proteins, cholesterol-linked and palmitoylated proteins [1–3]. Membrane rafts compartmentalize important cellular processes such as cell adhesion and endocytosis and have been proposed as signal transduction platforms and as key regulators of several signaling pathways [3–5].

One of the first methods originally used for the study of these domains was based on their insolubility in non-ionic detergent such as Triton X-100 [6]. These detergent-resistant membranes (DRMs) can be isolated from most mammalian cells. DRMs, like membrane rafts, are also rich in Chol and sphingolipids and are in the liquid-ordered phase. Moreover, the tight acyl chain packing and the enrichment in sphingomyelin (SM) and Chol are probably responsible for their detergent insolubility [7,8]. In spite of the existence of detergent-free methods and modern microscopy techniques, isolation of DRMs is still one of the most widely used methods for studying certain properties of membrane rafts. Certainly there remains a large degree of controversy surrounding the purity, the physiological importance, and even the existence of DRM in intact cells [9]. It is also possible that DRM preparations do not reflect the exact composition of the membrane rafts in intact cells, however, the purification of such domains has led to significant progress in understanding the functional architecture of biological membranes and in the dissection of signal transduction pathways [10].

DRM localization of phosphatidylinositol 4,5-bisphosphate (PIP_2)-metabolizing enzymes, several isoforms of PIP_2 specific phospholipase C (PLC), as well as phospholipase D (PLD) suggests a specific role of these specialized microdomains in lipid signaling [11–16].

Lipid messengers are generated by the concerted action of phospholipases and lipid kinases on membrane phospholipids. Phosphatidylcholine (PC), the most abundant glycerophospholipid in the membrane, plays a key role in cellular signaling since it is the main substrate for several signaling enzymes such as: PLD, phospholipase C (PC-PLC) and PLA^2 [17–19]. Phosphatidic acid (PA) generated by PLD

* Corresponding author. Tel.: +54 291 4861201; fax: +54 291 4861200.
E-mail address: salvador@criba.edu.ar (G.A. Salvador).

0005-2736/$ – see front matter © 2010 Elsevier B.V. All rights reserved.
doi:10.1016/j.bbamem.2009.12.008

can be further hydrolyzed by lipid phosphate phosphatases (LPPs) to generate the lipid second messenger diacylglycerol (DAG). Besides, DAG derived from PC can be generated by PC-PLC action. The wave of DAG elicited from PC hydrolysis is generated more slowly than that reported for PIP_2-PLC activity and it occurs without elevation of intracellular Ca^{2+}.

The coexistence of PLD and PC-PLC pathways has already been reported in cerebral cortex synaptic endings specific, sites heavily concentrated in signaling molecules [20]. Moreover, the synaptic endings appear to be the first target of neuronal damage in several neurodegenerative disorders. In this sense, the identification and characterization of signaling pathways have gained priority in order to understand how synaptic signaling operates both under normal and/or pathological conditions. We have also reported the activation of synaptic PLD and PC-PLC pathways under oxidative stress conditions and a differential regulation of PLD during aging [21–23].

In this work, we characterized the lipid and protein composition of synaptic endings and of DRMs obtained from cerebral cortex synaptic endings isolated from adult (4 month old) and aged (28 month old) rats. We also described for the first time the presence and the differential localization of PC-derived signaling pathways (PC-PLC and PLD) in these specialized microdomains.

2. Materials and methods

Wistar-strain adult (4 months old) and aged (28 months old) rats were kept under constant environmental conditions and fed on a standard pellet diet ad libitum until decapitation.

1-[^{14}C]palmitoyl-2-[^{14}C]palmitoyl-*sn*-glycero-3-phosphocholine ([^{14}C]-DPPC) (111 mCi/mmol), was purchased from New England Nuclear-Dupont, Boston, MA, USA. Preblended dry fluor 2a70 (98% PPO and 2% bis–MSB) was obtained from Research Products International Corp., USA. Triton X-100 (octyl phenoxy polyethoxyethanol), GTPγS (Guanosine 5′-[*gamma*-thio]triphosphate) and DL-propranolol were obtained from Sigma-Aldrich St. Louis, MO, USA. The kit (Colestat enzimático AA) for measuring cholesterol was from Wiener laboratory, Rosario, Argentina. The kit for measuring protein content (DC protein assay) was from Bio-Rad Life Science group. Rabbit polyclonal anti-Caveolin 1 antibody was from BD Biosciences, rabbit polyclonal anti-PLD1 antibody was from Cell Signaling, mouse monoclonal anti-c-Src antibody, polyclonal anti-Flotillin-1 antibody, polyclonal horse radish peroxidase (HRP)-conjugated goat anti-rabbit IgG and polyclonal HRP-conjugated goat anti-mouse IgG were purchased from Santa Cruz Biotechnology, Inc. (Santa Cruz, CA, USA). Anti-PLD2 was a kind gift from Dr. Raben, Johns Hopkins University School of Medicine, Baltimore, USA. Rabbit polyclonal anti-PC-PLC antibody raised against *Bacillus cereus* PC-PLC was generously provided by Dr. Goldfine, University of Pennsylvania, Philadelphia, USA. All other chemicals were of the highest purity available.

2.1. Preparation of synaptosomal fraction

Total homogenates were prepared from the cerebral cortex (CC) of 4 month old (adults) and 28 month old (aged) rats. Rats were killed by decapitation and CC was immediately dissected (2–4 min after decapitation). All proceedings were in accordance with *Principles of Use of Animals* and *Guide for the Care and Use of Laboratory Animals* (NIH regulation).

Synaptosomal fraction (Syn) was obtained as previously described by Cotman with slight modifications [22,24]. Briefly, CC homogenate (20%, w/v) was prepared in a medium containing 0.32 M sucrose, 1 mM EDTA, 10 mM HEPES buffer (pH 7.4) in the presence of 1 mM DTT, 2 μg/ml leupeptin, 1 μg/ml aprotinin, 1 μg/ml pepstatin, and 0.1 mM PMSF. The cerebral cortex was homogenized by 10 strokes with a Thomas tissue homogenizer. The homogenate was centrifuged at 1800×*g* for 7.5 min at 4 °C using a JA-21 rotor in a Beckman J2-21 centrifuge. The pellet was discarded, and the supernatant was retained and centrifuged at 14,000×*g* for 20 min at 4 °C. The resulting pellet was washed and resuspended in 3 ml of 0.32 M sucrose isolation buffer, layered over a discontinuous ficoll gradient (8.5% pH 7.4, 13% pH 7.4 ficoll solutions, each prepared in isolation buffer) and spun at 85,500 *g* for 30 min at 4 °C using a SW 28.1 rotor in a Beckman Optima LK-90 ultracentrifuge. Synaptosomes in the 8.5%–13% ficoll interface were removed, resuspended in isolation buffer, and centrifuged at 33,000×*g* for 20 min at 4 °C using a JA-21 rotor in a Beckman J2-21 centrifuge. For the experiments, synaptosomes were diluted in Tris base buffer medium (TBM) containing: 120 mM NaCl, 5.0 mM KCl, 1.0 mM $MgCl_2$, 5 mM $NaHCO_3$, 1.2 mM Na_2HPO_4, 10 mM glucose, 20 mM Tris (pH 7.2) and protein content was determined by a previously published method [25] using the DC protein assay kit from Bio-Rad.

2.2. Isolation of detergent-resistant membranes (DRMs)

The isolation of the DRM fraction from entire synaptosomes was based on the procedure previously described by Brown and Rose and by Molander-Melin et al. [6,26], with slight modifications to our experimental system. Briefly, the synaptosomal pellet obtained from 3 CC was resuspended in 5 ml of iced-cold (0–4 °C) lysis buffer consisting of 1% Triton X-100 in DRM buffer (10 mM Tris–HCl (pH 7.4), 70 mM NaCl, 2 mM $MgCl_2$ and 0.5 mM EDTA) with protease inhibitors added (1 mM DTT, 2 μg/ml leupeptin, 1 μg/ml aprotinin, 1 μg/ml pepstatin, and 0.1 mM PMSF). The suspension was homogenized by passing it through a 21 ga×1.5 in. needle 4–5 times and it was incubated at 4 °C for 30 min. The homogenization was repeated after 15 min of incubation. Then, the homogenate was centrifuged at 1000×*g* for 15 min at 4 °C (2500 rpm, Beckman JA-21 rotor, Beckman J2-21 centrifuge). The supernatant was diluted 1:1 in 80% (w/v) sucrose, divided into two samples and placed at the bottom of ultracentrifuge tubes. On top of this, 20 ml of 30% (w/v) sucrose were layered, followed of 8 ml 5% (w/v) sucrose. All the sucrose solutions were handled at 0–4 °C and diluted in the DRM buffer (without Triton X-100) containing protease inhibitors (1 mM DTT, 2 μg/ml leupeptin, 1 μg/ml aprotinin, 1 μg/ml pepstatin, and 0.1 mM PMSF). Samples were centrifuged for 20 h at 120,000×*g* (27,000 rpm, Beckman SW 28 rotor in a Beckman Optima LK-90 ultracentrifuge) at 4 °C. A visible and floating band (present in the 5–30% sucrose interface) was collected and transferred to a new centrifuge tube, which was filled up with DRM buffer and centrifuged for 1 h at 120,000×*g*. The pellet containing DRMs was resuspended in TBM buffer and protein content was determined by a previously published method [25] using the DC protein assay kit from Bio-Rad.

2.3. Determination of DAG generation from PC

PC hydrolysis was determined using lipid vesicles containing [^{14}C]-DPPC and cold DPPC to yield 100,000 dpm and 0.125 mM per assay in a buffer containing 0.2% Triton X-100 and 0.1 M Tris (pH 7.2). 100 μl of these lipid vesicles were added to 100 μl of Syn or DRMs (150 μg of protein) in a final volume of 200 μl. The reaction was carried out at 37 °C for 20 min and stopped by the addition of 5 ml of chloroform: methanol (2:1, v/v). Blanks were prepared identically, except that membranes were boiled for 5 min before use. Lipids were extracted and separated as described below [20,21]. To evaluate the contribution of the PC-PLC and PLD pathways to total DAG formation, the enzyme reaction was carried out under control conditions (vehicle) and in the presence of 2% ethanol or 1.5 mM DL-propranolol [21,22,27].

2.4. Lipid separation

After the enzyme reaction lipids were extracted according to Folch [28]. Briefly, the lipid extract was washed with 0.2 volumes of 0.05%

$CaCl_2$ and the lower phase was obtained after centrifugation at 900×*g* for 5 min. Neutral lipids (NLs): monoacylglycerol (MAG), diacylglycerol (DAG), and free fatty acid (FFA) were then separated by one-dimensional thin-layer chromatography (TLC) using silica gel G plates (Merck) in a mobile phase consisting of hexane: diethyl ether: acetic acid (50:50:2.6, v/v). PC was retained at the spotting site. Lipids were visualized by exposure of the plate to iodine vapors and DAG spots were scraped off the plate and radioactivity was determined by liquid scintillation as previously described [27].

To analyze the phospholipid (PLs) composition, total lipids from synaptosomes and DRMs were extracted according to Bligh and Dyer [29]. Total PLs were separated from NLs by one-dimensional TLC on silica gel G plates using a mobile phase consisting of hexane: diethyl ether: acetic acid (80:20:1, v/v). Individual PLs were separated by two-dimensional TLC on silica gel H plates (Merck) using a mobile phase consisting of chloroform: methanol: ammonia (65:25:5, v/v) for the first dimension and chloroform: acetone: methanol: acetic acid: water (30:40:10:10:4, v/v) for the second one, as previously described by Rouser et al. [30].

To resolve and visualize neutral and polar lipids in the same plate, a three-solvent method was performed. The first solvent system was chloroform: methanol: ammonia (65:25:5, v/v) up to 3/4 of the plate, then the plate was turned 90° and Chol and ceramide (CM) standards were loaded in the other 1/4 of the plate. Then NLs were resolved using hexane: diethyl ether: acetic acid (60:40:2.3, v/v). Then, the plate was divided in two and a fragment of silica was removed to prevent the third solvent system from dragging the NLs that were already resolved. Finally, the third solvent system (chloroform: acetone: methanol: acetic acid: water, 30:40:10:10:4, v/v) was used to end the resolution of PLs.

2.5. Lipid phosphorus measurement

In order to determine lipid phosphorus (lipid P), PLs were visualized by exposure of the plate to iodine vapors and lipid P was determined in each spot (and previously in total lipid extracts) using the chemicals and reactions described by Rouser et al. [30].

2.6. Cholesterol measurement

Total cholesterol content was measured in aliquots of the lipid extracts corresponding to 5 μg lipid P, using a commercial kit (Colestat enzimático AA) from Wiener laboratory. The aliquots were dried under N_2 gas and resuspended in 100 μl of isopropyl alcohol, and then the manufacturer's instructions were followed. Briefly, the method is based on a series of enzyme reactions: first cholesterol esterase hydrolyzes cholesterol esters to cholesterol and FFA, then cholesterol oxidase oxidizes cholesterol to cholesten-3-one plus H_2O_2 which reacts with 4-aminophenazone to generate a red compound (quinonimine) that can be measured spectrophotometrically at 505 nm.

2.7. Fatty acid derivatization and gas–liquid chromatography (GLC)

To analyze the fatty acid composition, phospholipids were separated as described above and visualized under UV light after spraying the plates with an N_2-driven solution of dichlorofluorescein in methanol and spots were scraped off the plate. After visualization with dichlorofluorescein, lipids were eluted by thoroughly mixing this silica three times with chloroform: methanol: water (5:5:1, v/v) and centrifuging the samples. The three eluates were pooled, mixed with four volumes of water, and separated into phases, to recover the lipids in the organic phase. The solvents used in the preparative and analytical steps were HPLC-grade.

The fatty acid composition of the lipids was determined by GLC of their fatty acid methyl ester (FAME) derivatives. The methyl esters from the fatty acids esterified to glycerol were obtained by subjecting aliquots from the total polar lipid fraction or the isolated phospholipids to acid methanolysis, as described above (fatty acids that were amide-bound to sphingolipids were excluded from this preparation). The sphingolipid sphingomyelin was dried and treated (under N_2) with one volume of 0.5 N NaOH in anhydrous methanol at 50 °C for 10 min, to remove any potential lipid contaminant with ester-bound fatty acids. After mild alkaline treatment, one volume of chloroform and one volume of 0.5 N HCl were added, and the tubes were centrifuged to recover the organic phases. These samples were rapidly dried and the SM was separated once again by TLC using chloroform: methanol: acetic acid: 0.15 M NaCl (20:10:3.2:1, v/v).

The phospholipids were converted to methyl esters by placing the dry lipid samples overnight at 45 °C with one volume of 0.5 N H_2SO_4 in anhydrous methanol under N_2 in Teflon-lined, screw-capped tubes [31]. Methyl heneicosanoate was added as an internal standard for quantitative analysis. Before GLC, all of the methyl ester samples were purified by TLC using hexane: ethyl ether (95:5, v/v) on silica gel G plates that had been previously washed with methanol: ethyl ether (75:25, v/v). The methyl ester spots were located under UV light after spraying with dichlorofluorescein, scraped into tubes, and recovered into hexane after thoroughly mixing the silica support with methanol: water: hexane (1:1:1, v/v; three successive hexane extractions). The combined hexane extractions were dried, the methyl esters were dissolved, and aliquots of the methyl ester solutions were taken for analysis. Nitrogen gas was used to protect the samples throughout the procedures used and all the solvents used in the preparative and analytical steps were HPLC-grade.

A Varian 3700 gas chromatograph equipped with two (2 m×2 m) glass columns packed with 10% SP 2330 on Chromosorb WAW 100/120 (Supelco Inc., Bellefonte, PA) was used. The column oven temperature was programmed from 155 °C to 230 °C at a rate of 5 °C/min, and then kept at this final temperature for about 30 min. The injector and detector temperatures were set at 220 °C and 230 °C, respectively, and N_2 (30 ml/min) was the carrier gas. The fatty acid peaks were detected with flame ionization detectors, operated in the dual-differential mode, and quantified by electronic integration (using a Varian workstation).

2.8. Sodium dodecyl sulfate-polyacrylamide gel electrophoresis (SDS-PAGE) and Western blot (WB) assays

Samples were denatured with Laemmli sample buffer at 100 °C for 5 min [32]. Equivalent amounts of synaptosomal and DRM proteins (25 μg) from adult and aged animals were separated by sodium dodecyl sulfate-polyacrylamide gel electrophoresis (SDS-PAGE) on 10% polyacrylamide gels and then transferred to polyvinylidene fluoride (PVDF) membranes (Millipore, Bedford, MA) which were blocked with 5% non-fat dry milk in TTBS buffer [20 mM Tris–HCl (pH 7.4), 100 mM NaCl and 0.1% (w/v) Tween 20] for 2 h at room temperature (Salvador et al., 2005). Membranes were then incubated with primary antibodies [anti-Caveolin 1 (1:1000) for 2 h at room temperature, anti-c-Src (1:1000) overnight at 4 °C, anti-Flotillin-1 (1:500) 2 h at room temperature, anti-PLD1 (1:300) overnight at 4 °C and anti-PLD2 (1:300) overnight at 4 °C, anti-PC-PLC (1:100) overnight at 4 °C], washed three times with TTBS and then exposed to the appropriate HRP-conjugated secondary antibody (anti-rabbit or anti-mouse) for 2 h at room temperature. Membranes were washed again three times with TTBS and immunoreactive bands were detected by enhanced chemiluminescence (ECL, Amersham Biosciences) using standard X-ray film (Kodak X-Omat AR).

2.9. Detection of GM1 ganglioside

GM1 was detected by Slot Blot. Briefly, synaptosomal and DRM proteins (3 μg) were transferred to a nitrocellulose membrane using the Bio-Dot SF (Bio-Rad). The membrane was then incubated with

cholera toxin subunit B-HRP-conjugated (CTB-HRP, Sigma-Aldrich) for 1 h at room temperature using a 1:30,000 dilution. The GM1-CTB specific union was detected by enhanced chemiluminescence.

2.10. Detection of PC-PLC by Dot Blot assay

Equivalent amounts of synaptosomal and DRM proteins (2 μg) from adult and aged animals were transferred to a nitrocellulose membrane. The membrane was blocked and incubated with anti-PC-PLC antibody (1:100) for 2 h at room temperature. Then the membrane was incubated with the secondary antibody for 1 h at room temperature and immunoreactive spots were detected by enhanced chemiluminescence.

2.11. Statistical analysis

Statistical analysis was performed using two-way ANOVA followed by Bonferroni's test to compare means. *p*-values less than 0.05 were considered statistically significant.

3. Results

3.1. Characterization of DRMs isolated from cerebral cortex synaptic endings from adult and aged rats

DRMs can be isolated from membranes of different tissues and cell types mainly based on their detergent insolubility at low temperature and low buoyant density upon discontinuous sucrose density gradient centrifugation. We isolated DRMs from entire synaptic endings obtained from the individual cerebral cortex of 4 and 28 month old Wistar rats using 1% Triton X-100 at 4 °C [6,26]. After 20 h of centrifugation at 120,000×*g*, a visible band appeared in the interface of 5% and 30% sucrose. This band was named DRM and it was collected for the determination of lipid and protein content. Data obtained from DRMs were analyzed and compared to those obtained from whole synaptosomes, from adult as well as from aged rats.

Quantification of the DRM marker cholesterol show an enrichment of approx. 35% in this lipid in DRM membranes with respect to the values obtained from synaptic endings. Cholesterol content did not change when compared in DRMs from adult and aged animals (Fig. 1A). DRMs from adult and aged animals were also enriched in SM content by 120% and 66%, respectively (Fig. 1B). It is noticeable that SM content in Syn and DRMs obtained from aged rats was 79% and 36% higher than in Syn and DRMs from adults, respectively. The other raft lipid marker GM1 ganglioside was also studied by Slot blot experiments. However, there were no significant differences in GM1 content between Syn and DRM preparations (Fig 1E). DRMs are considered specialized domains rich in phospholipids (PLs) with a predominant saturated fatty acyl composition. Phospholipid/protein ratio was increased more than 3 times in DRMs with respect to Syn. This enrichment in PLs content was similar in adult and aged animals (Fig. 1C).

SDS-PAGE analysis of DRMs and Syn showed a differential protein profile. Proteins with a molecular weight of approximately 90, 60 and 20 kDa were absent in the DRM fraction, whereas 40 and 30 kDa proteins turned out to be more concentrated in the same fraction (Fig. 1D). Specific marker proteins for DRMs differ from cell to cell, however, most of Src-family tyrosine kinases are associated with DRMs. Using a monoclonal antibody against c-Src, a single 60 kDa band both in Syn and DRM preparations was detected by Western blot. c-Src was highly concentrated in the DRM fractions with respect to Syn. No differences in c-Src localization were observed when comparing adult versus aged animals (Fig. 1E). Additionally, Caveolin p21 (a specific marker for a subset of specialized microdomains) and Flotillin-1 were also enriched in DRMs from adult and aged rats (Fig. 1E). Flotillin-1 and 2 (originally discovered in neurons during axon regeneration) were independently identified as markers of membrane rafts in flotation assays [33–35]. In order to control the amount of protein loaded in each sample, membranes were stained with 0.5% Ponceau S in 1% acetic acid before the incubation with the primary antibodies.

3.2. Phospholipid composition of Syn and DRMs from adult and aged rats

TLC separation of total lipids from Syn and DRM fractions was performed using a three-solvent method as described in Section 2. Fig. 2A and B showed visible differences in the phospholipid profile between the two fractions. PC and SM spots were more stained in the DRM fraction. A spot with a Rf similar to that of ceramide (CM) standard was not detected in Syn fraction, but it was visualized in the DRM fraction (Fig. 2A and B, indicated with arrows).

Quantitative analysis of individual phospholipids scraped off the plate was performed by measuring lipid phosphorus (lipid P) as described by Rouser et al., [30]. Distribution of phospholipid classes in Syn and DRMs obtained from adult and aged rats is shown in Fig. 2C and D, respectively. PC and phosphatidylethanolamine (PE) were the major phospholipids in the Syn fraction. They represented 42% and 40% of the total Syn PLs, respectively. As minoritary PLs: phosphatidylserine (PS), SM, phosphatidylinositol (PI) and PA represented 10; 2,2; 1,6 and less than 0,5% of total PLs, respectively (Fig. 2C). No significant differences were observed in the percentage phospholipid distribution of Syn obtained from aged rats when compared with adults, except for SM, which was 80% higher in Syn from aged rats than that from adults (Fig. 2C and D).

Relative to Syn, DRM fraction was enriched in PC (by 28%) whereas PE and PS levels diminished (by approx. 25%) in adult rats. Phospholipid distribution in DRMs from aged animals did not show significant differences with respect to that observed in adults, except for SM content as previously mentioned (Fig. 1B). Regarding the parent Syn fraction, the DRM fraction had a higher PC/PE ratio (1.5 versus 1) both in adult and aged animals. DRMs from aged animals registered the highest SM/PC ratio value, (0.12) with respect to DRMs from adults (0.08) and entire Syn (0.05 and 0.09, respectively). This quantitative analysis confirmed the differences observed in the TLC plates between Syn and DRMs.

3.3. Phospholipids fatty acyl composition in Syn and DRMs obtained from adult rats

The fatty acid content of total PLs and of individual phospholipids in Syn and DRMs obtained from adult rat cerebral cortex are compared in Fig. 3. Total phospholipid-fatty acid composition from DMRs showed an increase in the saturated fatty acid, 16:0 (35%), and a decrease in the polyunsaturated fatty acids (PUFA), 20:4n-6, 22:4n-6 and 22:6n-3 content by 67%, 60% and 68%, respectively with respect to isolated Syn (Fig. 3A). The increase in 16:0 content and the dramatic decrease in PUFA were reflected in the fatty acyl composition of PC (Fig. 3B).

PE and PS from DRMs did not show any significant change in their fatty acyl composition when compared with Syn (Fig. 3C and D). SM showed an increase in 18:0 (19%) and 20:0 (27%) and a decrease in 16:0 (59%) (Fig. 3E), while PI only showed a decrease in 18:1 content (23%) with respect to Syn (Fig. 3F).

3.4. Phospholipid-fatty acid composition in Syn and DRMs obtained from aged rats

Fig. 4 shows the fatty acid content of total and individual phospholipids in Syn and DRMs obtained from aged rat cerebral cortex. Relative to Syn, DRM PLs from aged animals were enriched in 16:0 (34%) and showed a significant decrease (80%) in the content of 20:4n-6 and 22:6n-3 (Fig. 4A). The decrease in PUFA content observed in the total phospholipid fraction from DRMs was reflected in PC fatty

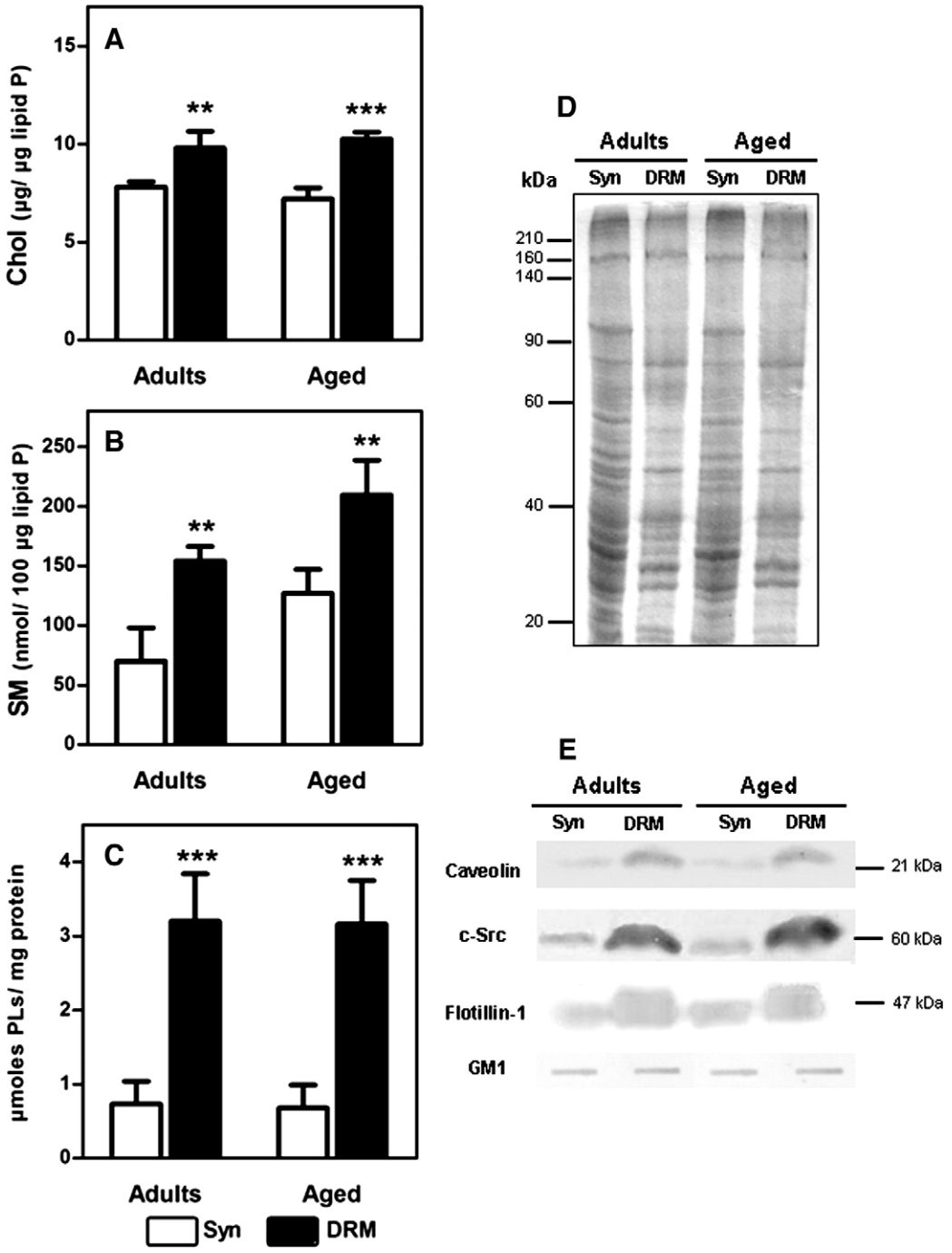

Fig. 1. Characterization of DRMs isolated from synaptic endings from adult and aged rat cerebral cortex. DRMs were obtained from isolated CC Syn from adult and aged rats by their relative insolubility in cold Triton X-100. Total lipids from Syn and DRMs were extracted according to Bligh and Dyer [29]. (A) Cholesterol content in Syn and DRMs: total cholesterol was measured in aliquots of the lipid extracts corresponding to 5 µg lipid phosphorus using an enzymatic method. Results are expressed as µg Chol/µg lipid P. (B) SM content in Syn and DRMs: SM was isolated from other phospholipids by two-dimensional TLC and quantified by determining the lipid P. Results are expressed as nmol/100 µg lipid P. (C) µmol of PLs per µg of protein ratio in Syn and DRMs. (D) Protein profile from Syn and DRMs: Syn and DRM proteins (25 µg) were resolved by SDS-PAGE on a 10% gel. Proteins were visualized by Coomassie blue staining. Numbers to the left indicate the molecular weights of commercial standards. (E) Caveolin, c-Src, Flotillin-1 and GM1 content in Syn and DRMs: to evaluate Caveolin, c-Src and Flotillin-1 presence, Syn and DRM proteins (25 µg) were resolved in a 10% SDS-PAGE and transferred to a PDVF membrane. Membranes were blocked, incubated with primary and secondary antibodies as detailed in Section 2. Immunoreactive bands were detected by enhanced chemiluminescence. Numbers to the right indicate molecular weights. GM1 content was evaluated by Slot blot: 3 µg of Syn and DRM proteins were transferred to a nitrocellulose membrane which was then incubated with CTB-HRP. For A, B and C: data represent the mean value ± SD of at least three independent experiments using a pool of three animals on each occasion. Results from Syn and DRMs were compared each experiment was performed three times in duplicate, using a pool of three animals on each occasion (***$p<0.001$; **$p<0.01$). For D and E: data shown is a representative result of three independent experiments. Detailed descriptions are found in the Section 2.

acyl composition where 20:4n-6 and 22:6n-3 diminished by 64% and 73% respectively (Fig. 4B). Moreover, SM was enriched in 18:0 and 20:0 in the DRM fraction (Fig. 4E). PI fatty acyl composition from DRM fraction presented also an increase in 16:0 content (46%) and a decrease in 20:4n-6 by 64% (Fig. 4F). Similarly to the observations made in adult animals, PE and PS did not show any difference in their fatty acid composition between Syn and DRMs from aged rats (Fig. 4C and D).

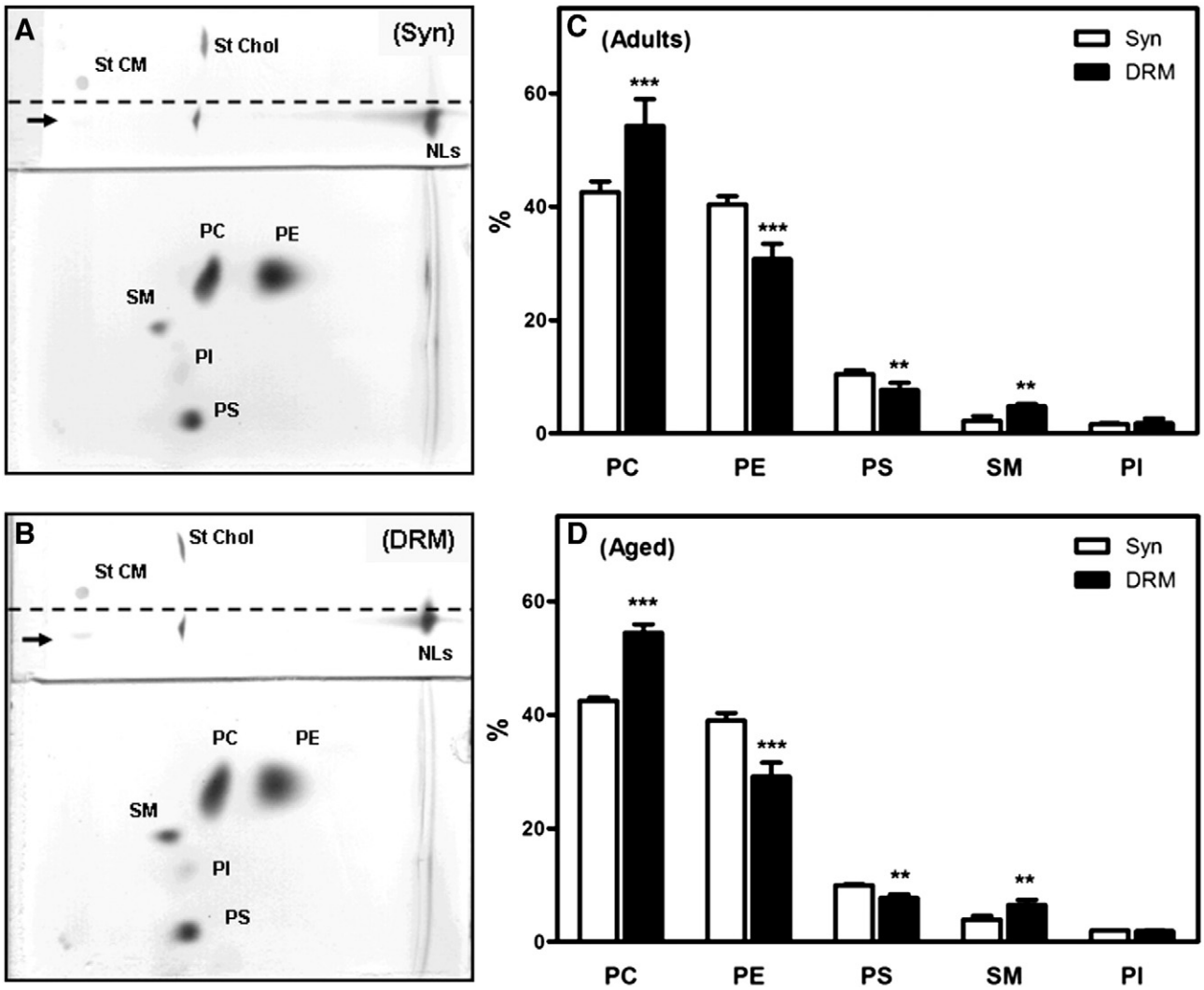

Fig. 2. Percentage phospholipid composition of Syn versus DRMs. Total lipids from Syn and DRMs from adult and aged rats were extracted as described in Fig. 1. Lipids (corresponding to 15 μg lipid P) were separated by TLC using a three-solvent system, individual lipids were revealed with iodine vapors, scraped and quantified by determining the lipid P of each spot. (A) TLC of Syn lipid extract. (B) TLC of DRM lipid extract. (C) Percentage phospholipid composition of Syn versus DRMs from adult animals. (D) Percentage phospholipid composition of Syn versus DRMs from aged animals. Detailed descriptions are found in the Section 2. Data represent the mean value ± SD of at least three independent experiments using a pool of three animals on each occasion. Results from Syn and DRMs were compared (***$p < 0.001$; **$p < 0.01$).

3.5. Age-associated changes in phospholipid-fatty acyl composition of Syn and DRMs

Tables 1 and 2 show the detailed fatty acyl composition from total and individual PLs in Syn and DRMs obtained from adult and aged rats. Compared to adults, Syn from aged animals presented a dramatic decrease in 20:4n-6 and 22:6n-3. In the total PL fraction from Syn 20:4n-6 content diminished by 54% whereas 22:6n-3 decreased by 62%. These changes were reflected in the PUFA content and the unsaturation index (UI) that diminished by 58% and 50%, respectively (Table 1). Compared to adults, the Syn PLs from aged animals that presented the most dramatic diminution in the 22:6n-3 content were PS, PC and PE (70%, 42% and 32%, respectively. See Tables 1 and 2). Syn PI from aged animals presented the most striking diminution (by 50%) in 20:4n-6 content when compared with the values found in adults. PC and PE showed a minor but significant decrease in 20:4n-6 content (31 and 21%, respectively) in aged Syn.

Regarding DRM fraction from aged animals, total phospholipids presented a significant decrease in 20:4n-6 and 22:6n-3 when compared to DRMs from adults (Table 1). These differences are also reflected in the decrease of PUFA content and in the UI in DRMs from aged rats (71 and 65%, respectively). With respect to adults, 18:1 content only decrease in the DRM fraction from aged animals while no differences were seen in entire Syn (Table 1). The greatest difference between DRMs from adult and aged animals was the 5-fold decrease in 22:6n-3 in PS in DRMs from aged animals over DRMs from adults (Table 2). Similar results were observed in PI 20:4n-6 content that presented 4-fold decrease in DRM from aged over DRMs from adult animals (Table 2). SM did not show any age-associated change in its fatty acid composition, both in Syn as well as in DRMs.

3.6. Localization of PC- derived signaling pathways in DRMs and Syn

In order to study the localization of PC hydrolyzing enzymes WB assays were performed in DRM and Syn obtained from adult and aged animals. Fig. 5A shows that PLD1 isoform is highly enriched in DRM from adult and aged rats when compared to isolated synaptic endings. On the contrary, PLD2 is excluded from the DRM fraction from adults as well as from aged rats (Fig. 5A).

Although the molecular structure of eukaryotic PC-PLC is still lacking, it was demonstrated that antibodies prepared to *Bacillus cereus* PC-PLC cross-react with a PC-PLC from mammalian cells

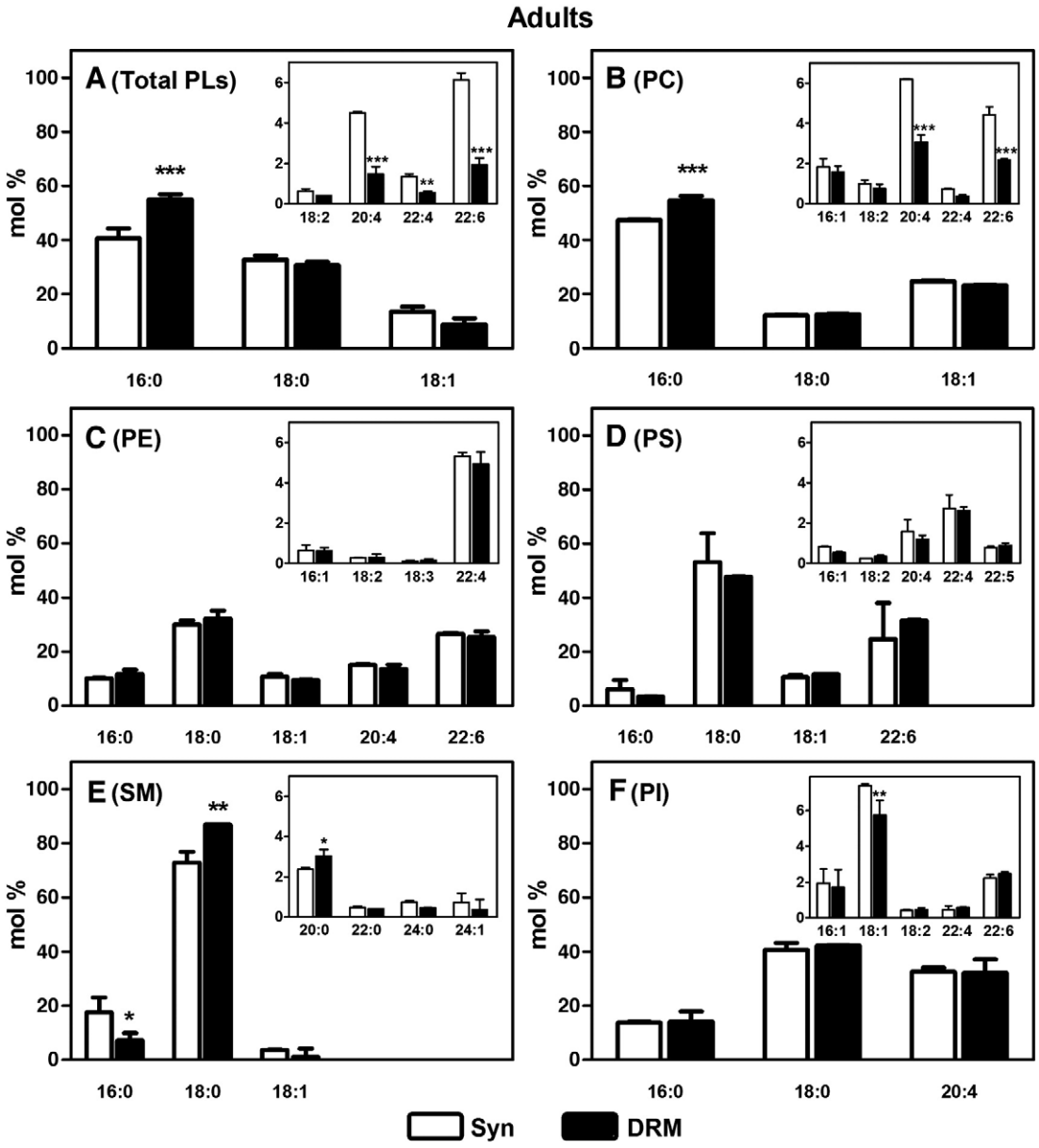

Fig. 3. Comparison of fatty acid composition of total and individual phospholipids between Syn and DRMs from adult rats. Total lipids from Syn and DRMs from adult rats were extracted as described in Fig. 1. Phospholipids (corresponding to 50 μg lipid P) were separated, isolated and derivatised as described in Section 2. FAME derivatives were analyzed by GLC. (A) Total PLs fatty acid composition. (B) PC fatty acid composition. (C) PE fatty acid composition. (D) PS fatty acid composition. (E) SM fatty acid composition. (F) PI fatty acid composition. Detailed descriptions are found in the Section 2. Results are expressed as mol% and data represent the mean value ± SD of at least three independent experiments using a pool of three animals on each occasion. Results from Syn and DRMs were compared (***$p<0.001$; **$p<0.01$; *$p<0.05$).

[20,36–38]. The detection of synaptosomal PC-PLC by Western blot assay using a polyclonal antibody raised against the bacterial PC-PLC showed two close bands corresponding to 66 kDa in Syn from adult and aged rats (Fig. 5B). *Clostridium perfringens* PC-PLC (PC-PLC$_{Cp}$) was used as a positive control for the antibody since the N-terminal domain of this protein shows structural similarity to *B. cereus* PC-PLC [39]. Dot blot assays showed that PC-PLC is also enriched in DRMs from adult and aged animals with respect to synaptosomes (Fig. 5C).

3.7. DAG generation from PC in DRMs and Syn

We have previously reported that DAG generated from PC can be produced by PLD and PC-PLC activities in synaptic endings [20,21]. As it has been extensively reported, in the presence of primary alcohols PLD exclusively catalyzes a transphosphatidylation reaction yielding phosphatidylalcohols instead of PA [40,41]. For this reason, to study the contribution of synaptic PC-PLC and PLD pathways to DAG generation, ethanol was included in the enzyme assays. Under these experimental conditions, the generation of phosphatidylalcohols blocks LPPs action and allows the measurement of DAG generation exclusively from PC-PLC activity [20,21]. Moreover, besides its β-adrenergic antagonist effect, DL-propranolol is also able to inhibit LPPs activity when it is used in high concentrations [17,42,43] (See the schema in Fig. 6A).

Fig. 6B shows that in Syn from adult and aged rats, [^{14}C]-DAG formation from [^{14}C]-DPPC was reduced by 35% when the enzyme reaction was carried out in the presence of 2% ethanol. This result demonstrates that in the synaptic endings about 35% of DAG generated from PC is due to PLD/LPP pathway and 65% is due to PC-PLC activity. A similar decrease was observed when Syn were incubated with 1.5 mM DL-propranolol, confirming the contribution of PLD/LPP pathway. Conversely, in the DRM fraction DAG formation

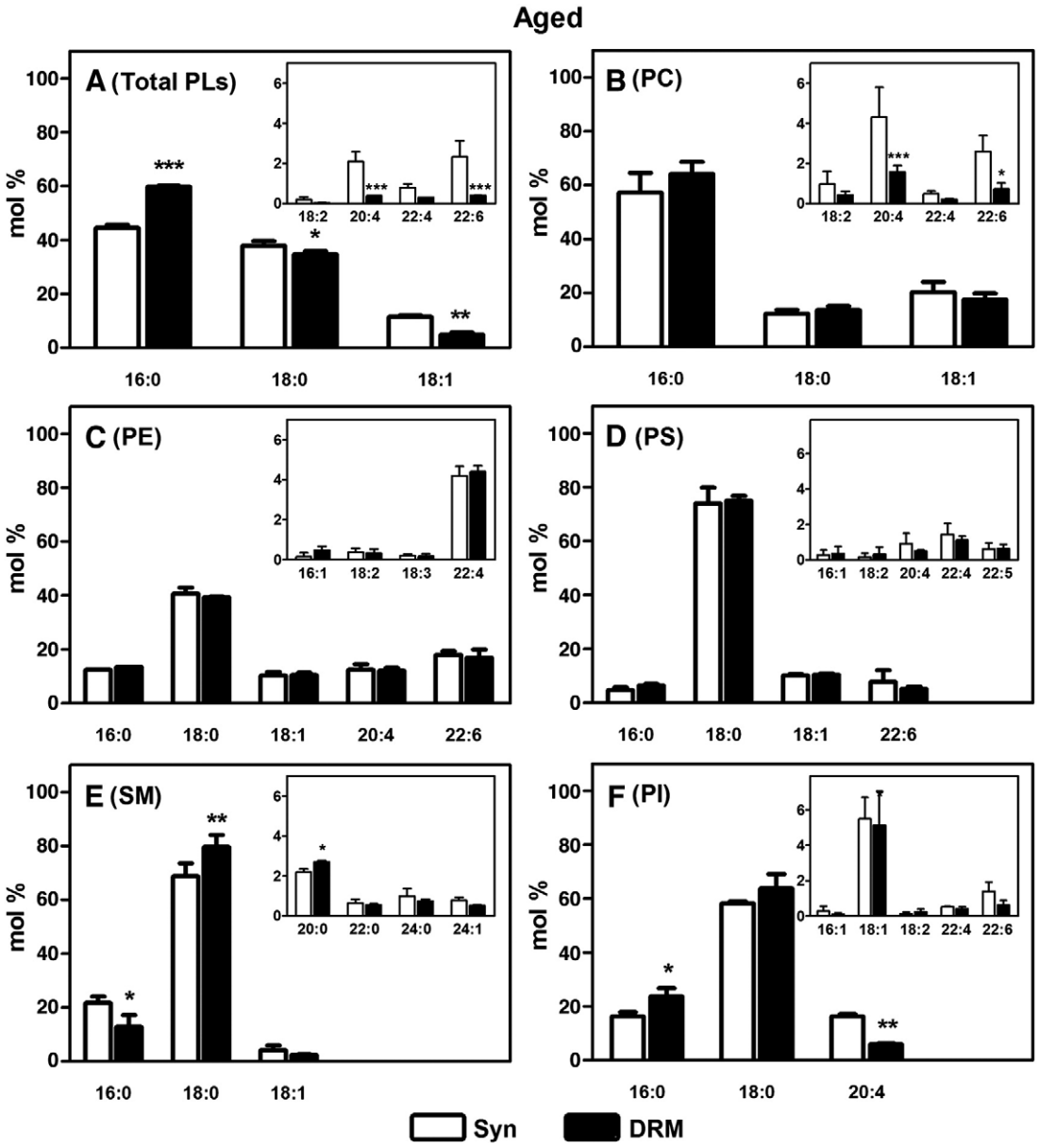

Fig. 4. Comparison of fatty acid composition of total and individual phospholipids between Syn and DRMs from aged rats. Total lipids from Syn and DRMs from aged rats were extracted, treated and analyzed as described in Fig. 3. (A) Total PLs fatty acid composition. (B) PC fatty acid composition. (C) PE fatty acid composition. (D) PS fatty acid composition. (E) SM fatty acid composition. (F) PI fatty acid composition. Detailed descriptions are found in the Section 2. Results are expressed as mol% and data represent the mean value ± SD of at least three independent experiments using a pool of three animals on each occasion. Results from Syn and DRMs were compared (***$p<0.001$; **$p<0.01$; *$p<0.05$).

did not decrease in the presence of ethanol, in spite of the enrichment in PLD1 in the detergent-resistant fraction (Fig. 6C). Therefore, under our experimental conditions, no PLD activity was detected in DRMs. On the other hand, PC-PLC specific activity (measured as DAG generation in the presence of ethanol) was 76 ± 20% and 45 ± 16% higher in DRMs compared to Syn from adult and aged rats, respectively (Fig. 7A). It is important to note that no significant differences in PC-PLC activity were observed between adults and aged animals, in Syn as well as in the DRM fraction.

As it is well known, GTPγS stimulates PLD1 by activating small G-proteins that can modulate the enzyme activity [44,45]. In this regard, the presence of 100 μM GTPγS plus ethanol allowed us to evaluate DAG generation under optimal PLD1 activity conditions. Fig. 7B shows that in DRMs isolated from adult rats [^{14}C]-DAG levels were not modified in the presence of 100 μM GTPγS plus ethanol with respect to the control condition. However, the presence of 100 μM GTPγS plus 2% ethanol decreased by 28% the DAG generation from PC in DRMs from aged animals (Fig. 7B). The presence of 100 μM GTPγS alone did not modified DAG generation with respect to the control condition (data not shown). This result suggests the activation of PLD1 only in DRM isolated from aged animals (See schema in Fig. 7C).

4. Discussion

In this work we present evidence for the distinct composition of Syn and DRM fractions obtained from adult and aged animals. We also demonstrate a differential localization of PC-PLC and PLD isoforms in DRMs and entire Syn.

The DRM fraction obtained from the CC synaptic endings presented typical characteristics of membrane rafts like the higher content of SM and Chol and the enrichment in Caveolin, c-Src and Flotillin-1, three proteins widely used as markers of membrane rafts [5,33–35,46–48]. GM1 ganglioside was present in Syn as well as in DRMs. However, no

Table 1
Comparison of fatty acid composition of total PLs, PC and PE from adult and aged rats. Fatty acid composition was analyzed as described in Fig. 3. Results are expressed as mol% and data represent the mean value ± SD of at least three independent experiments using a pool of three animals on each occasion. Results from adult and aged rats were compared (***$p<0.001$; **$p<0.01$; *$p<0.05$). Unsaturation Index (UI), defined as Σ (number of double bonds in each fatty acid) × (mol% of each fatty acid).

	Syn		DRM	
	Adults	Aged	Adults	Aged
Total PLs				
16:0	40.62 ± 3.65	44.64 ± 1.20	**54.92 ± 1.97**	**59.81 ± 0.32****
16:1	Nd	Nd	Nd	Nd
18:0	**32.75 ± 1.50**	**37.85 ± 1.73***	**30.60 ± 1.26**	**34.75 ± 1.12***
18:1	13.63 ± 1.74	11.48 ± 0.62	**8.92 ± 2.18**	**4.83 ± 0.88***
18:2n-6	0.61 ± 0.14	0.18 ± 0.14	0.39 ± 0.01	0.2 ± 0.01
18:3n-6	Nd	Nd	Nd	Nd
20:4n-6	**4.51 ± 0.04**	**2.08 ± 1.05*****	**1.48 ± 0.36**	**0.38 ± 0.01*****
22:4n-6	1.35 ± 0.13	0.78 ± 0.29	0.54 ± 0.08	0.29 ± 0.01
22:5n-6	Nd	Nd	Nd	Nd
22:6n-3	**6.13 ± 0.35**	**2.33 ± 1.43*****	**1.94 ± 0.32**	**0.39 ± 0.01*****
MUFA	13.63 ± 1.74	11.48 ± 0.62	**8.92 ± 2.18**	**4.83 ± 0.88****
PUFA	**12.60 ± 0.38**	**5.37 ± 2.91****	**4.35 ± 0.75**	**1.26 ± 0.04***
UI	**75.06 ± 4.23**	**37.26 ± 14.84*****	**29.42 ± 5.84**	**10.25 ± 1.04*****
PC				
16:0	**47.22 ± 0.34**	**57.23 ± 7.39*****	**54.64 ± 1.60**	**64.20 ± 4.42*****
16:1	**1.83 ± 0.40**	**Nd****	**1.58 ± 0.28**	**Nd*****
18:0	12.18 ± 0.26	12.29 ± 1.45	12.58 ± 0.13	13.68 ± 1.32
18:1	**24.65 ± 0.38**	**20.24 ± 3.85***	**23.06 ± 0.27**	**17.59 ± 2.25*****
18:2n-6	0.98 ± 0.19	0.97 ± 0.63	0.77 ± 0.19	0.42 ± 0.19
20:4n-6	**6.19 ± 0.03**	**4.31 ± 1.49****	**3.05 ± 0.37**	**1.56 ± 0.33*****
22:4n-6	0.74 ± 0.07	0.47 ± 0.15	0.38 ± 0.06	0.19 ± 0.04
22:6n-3	**4.42 ± 0.39**	**2.59 ± 0.80****	**2.18 ± 0.04**	**0.72 ± 0.29*****
PE				
16:0	**10.10 ± 0.26**	**12.48 ± 0.12***	11.75 ± 1.53	13.48 ± 0.01
16:1	0.63 ± 0.27	0.14 ± 0.20	0.61 ± 0.17	0.48 ± 0.20
18:0	**30.00 ± 1.55**	**40.58 ± 2.28*****	**32.23 ± 2.92**	**39.29 ± 0.36*****
18:1	10.71 ± 1.08	10.33 ± 1.32	9.48 ± 0.21	10.48 ± 0.94
18:2n-6	0.27 ± 0.01	0.37 ± 0.21	0.29 ± 0.16	0.32 ± 0.21
18:3n-6	0.10 ± 0.04	0.20 ± 0.08	0.15 ± 0.07	0.17 ± 0.13
20:4n-6	**15.14 ± 0.21**	**12.51 ± 2.04***	13.55 ± 1.65	12.08 ± 1.14
22:4n-6	**5.33 ± 0.19**	**4.19 ± 0.48*****	4.93 ± 0.61	4.40 ± 0.30
22:6n-3	**26.51 ± 0.50**	**18.04 ± 1.32*****	**25.41 ± 2.05**	**16.91 ± 3.11*****

Bold data are used in order to highlight significant results.

Table 2
Comparison of fatty acid composition of total PS and PI from adult and aged rats. Fatty acid composition was analyzed as described in Fig. 3. Results are expressed as mol% and data represent the mean value ± SD of at least three independent experiments using a pool of three animals on each occasion. Results from adult and aged rats were compared (***$p<0.001$; **$p<0.01$; *$p<0.05$).

	Syn		DRM	
	Adults	Aged	Adults	Aged
PI				
16:0	**13.78 ± 0.29**	**16.18 ± 1.61***	**14.14 ± 3.75**	**23.68 ± 3.07*****
16:1	**1.93 ± 0.79**	**0.27 ± 0.30****	1.71 ± 0.97	0.1 ± 0.07
18:0	**40.70 ± 2.56**	**58.26 ± 0.72*****	**42.27 ± 0.23**	**63.73 ± 5.34*****
18:1	**7.39 ± 0.11**	**5.50 ± 1.21****	5.73 ± 0.82	5.12 ± 1.92
18:2n-6	0.41 ± 0.05	0.12 ± 0.12	0.45 ± 0.11	0.23 ± 0.16
20:4n-6	**32.66 ± 1.46**	**16.24 ± 0.90*****	**32.16 ± 5.02**	**5.85 ± 0.49*****
22:4n-6	0.44 ± 0.23	0.52 ± 0.04	0.57 ± 0.03	0.40 ± 0.13
22:6n-3	2.23 ± 0.19	1.39 ± 0.52	**2.44 ± 0.12**	**0.62 ± 0.27***
PS				
16:0	6.16 ± 3.29	4.71 ± 1.04	**3.36 ± 0.17**	**6.37 ± 0.67*****
16:1	0.82 ± 0.02	0.27 ± 0.30	0.53 ± 0.04	0.36 ± 0.40
18:0	**52.24 ± 10.64**	**73.95 ± 5.87*****	**47.67 ± 0.15**	**74.95 ± 1.83*****
18:1	10.53 ± 0.90	10.10 ± 0.59	11.62 ± 0.10	10.37 ± 0.60
18:2n-6	0.23 ± 0.01	0.16 ± 0.20	0.33 ± 0.07	0.32 ± 0.40
20:4n-6	1.57 ± 0.60	0.91 ± 0.60	**1.20 ± 0.19**	**0.49 ± 0.08*****
22:4n-6	2.74 ± 0.66	1.44 ± 0.62	2.61 ± 0.19	1.11 ± 0.23
22:5n-6	0.78 ± 0.06	0.61 ± 0.35	0.88 ± 0.12	0.63 ± 0.25
22:6n-3	**24.61 ± 13.39**	**7.72 ± 4.44****	**31.49 ± 0.36**	**5.09 ± 0.95*****

Bold data are used in order to highlight significant results.

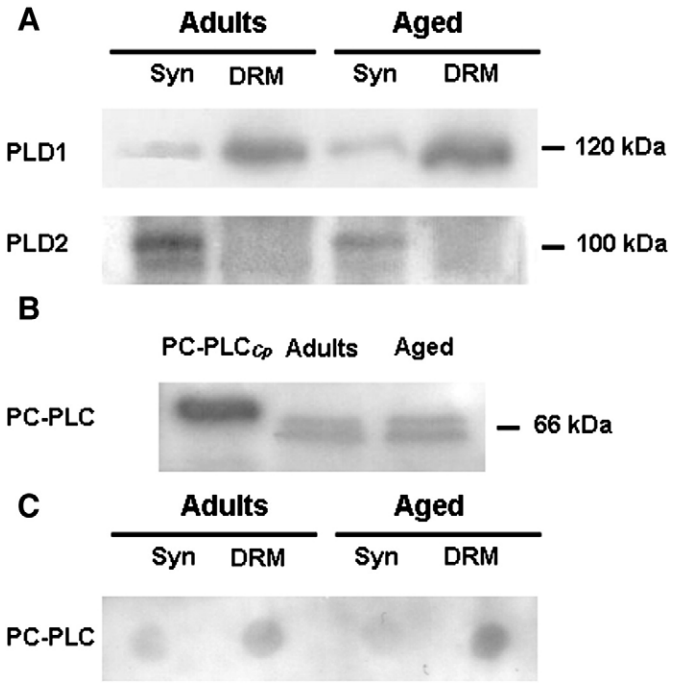

Fig. 5. Localization of PC-derived signaling pathways in DRMs and Syn. (A) PLD isoforms localization: Syn and DRM proteins (25 μg) were resolved in a 10% SDS-PAGE and transferred to a PDVF membrane. Membranes were blocked, incubated with primary (anti-PLD1 or anti-PLD2) and secondary antibodies as detailed in Section 2. Immunoreactive bands were detected by enhanced chemiluminescence. Numbers to the right indicate molecular weights. (B) Determination of synaptosomal PC-PLC by WB: Syn proteins (25 μg) were resolved in a 10% SDS-PAGE and transferred to a PDVF membrane. Membranes were blocked and incubated with the primary and secondary antibodies as detailed in Section 2. (C) PC-PLC localization: Syn and DRM proteins (2 μg) were transferred to a nitrocellulose membrane. Membranes were blocked, incubated with the primary and secondary antibodies as detailed in Section 2. Data shown is a representative result of three independent experiments.

difference in this ganglioside content was detected between the two fractions. This fact could be due to the high levels of gangliosides present in the nervous system membranes [8,26].

Compared to Syn, the detergent-resistant fraction showed and enrichment in PC and SM and a decrease in PE and PS, both in adult and aged animals. A similar phospholipid distribution was observed in DRMs obtained from photoreceptor outer segments [49] and the enrichment in PC content was also seen in membrane rafts isolated from whole rat brains [50].

The highly saturated lipid environment of membrane rafts favors the localization of proteins acylated with saturated fatty acids including G-protein α, Src-family tyrosine kinases and caveolins [51]. DRM fraction obtained from CC Syn presented a more saturated fatty acid composition than synaptosomes, with a great decrease in the PUFA content and in the UI. These changes in the total PLs acyl composition were probably mainly due to the acyl composition of PC. Nevertheless, it cannot be discarded that differences in the relative phospholipid abundance between Syn and DRMs could be also contributing to the more saturated composition of the DRM fraction, since the percentage of the most unsaturated phospholipids (PE and PS) is decreases in DRMs with respect to entire Syn. A similar profile in the fatty acid composition was observed in DRMs obtained from photoreceptor outer segments [49].

Brain aging is characterized by the decline of several physiological functions and it is accompanied by changes in the overall composition of membrane lipids that initiate alterations in the physicochemical properties of biological membranes [52–54]. No age-associated differences were observed in the phospholipid composition of the synaptic endings or the DRM fraction, with the exception of SM content. Similar results were also previously reported in the whole rat cerebral

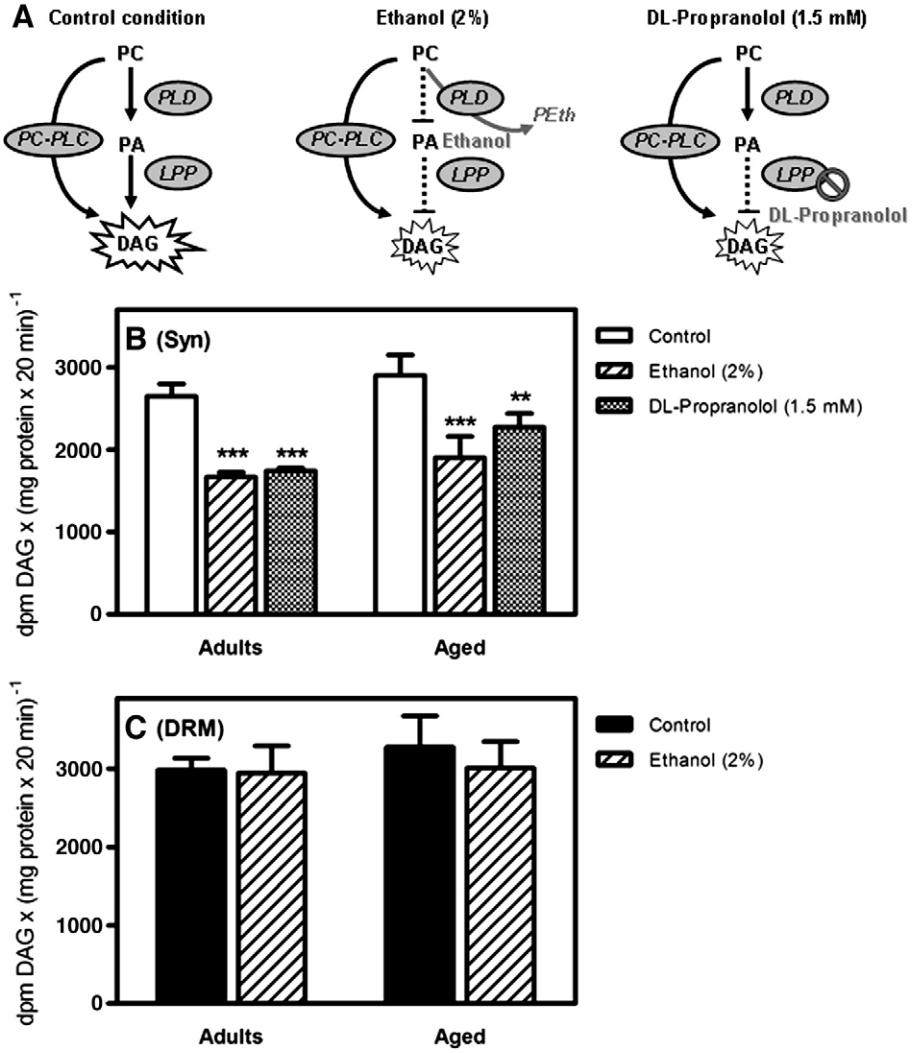

Fig. 6. DAG generation from PC in DRMs and Syn. (A) Schematic view of DAG generation under the different experimental conditions. Full arrows indicate active pathways while dotted lines indicate non active or inhibited pathways. (B) Syn from adult and aged rats were resuspended in Tris base buffer medium (TBM). The enzyme reaction was started by adding 100 µl synaptosomal suspensions (150 µg proteins) to 100 µl of lipid vesicles (containing [^{14}C]-DPPC and non-radiolabeled DPPC to yield 100,000 dpm and 0.125 mM per assay) in the presence of vehicle (control condition), 2% ethanol or 1.5 mM DL-Propranolol. After 20 min incubation at 37 °C, the enzyme reaction was stopped, lipids were extracted and isolated and [^{14}C]-DAG quantified as described in Section 2. (C) DRMs from adult and aged rats were resuspended in TBM and the enzyme reaction was carried out as described in Fig. 6B in the presence of vehicle (control condition) or 2% ethanol. Results are expressed as dpm DAG × (mg protein × 20 min)$^{-1}$ and were compared to the control condition. Data represent the mean value ± SD of at least three independent experiments using a pool of three animals on each occasion (***$p < 0.001$; **$p < 0.01$).

cortex obtained from adult and aged rats [52,55]. However, SM content also increased in the cerebral hemispheres from aged rats [56].

The drastic changes in the fatty acid composition observed in total and individual PLs of Syn and DRMs from aged animals, were mainly due to a huge decrease in PUFA (20:4n-6 and 22:6n-3). In previous work from our laboratory it was showed that 20:4n-6 (arachidonic acid) and 22:6n-3 (docosahexaenoic acid) content had also decreased in lipids isolated from the entire cerebral cortex from aged rats [55]. Noticeably, results presented here demonstrated that aged animals underwent a dramatic decrease in PUFA content in Syn and DRM fractions. Our results show that changes in 20:4n-6 content were observed in PC and PE but mostly in PI, and were even more pronounced in PI from aged rats DRM. This decrease in arachidonic acid (AA) could induce changes in arachidonic-derived signaling in the synaptic endings during aging.

Docosahexaenoic acid (DHA), in particular, is the most abundant polyunsaturated fatty acid in the brain, essential for optimal neuronal and retinal function, and PS contains an exceptionally high proportion of this fatty acid [57,58]. In neural cells, DHA influences vital signaling events in neuronal survival and differentiation [58,59]. Moreover, transformation of DHA to Neuroprotectin D1 (NPD1) rescues neuronal cells from cell death under pathological conditions. It has been also indicated that low levels of DHA in the brain are associated with neurodegenerative diseases, such as generalized peroxisomal disorders [60] and Alzheimer's disease [61]. Furthermore, it was demonstrated that DHA prevents neuronal apoptosis by facilitating Raf-1 and Akt translocation/activation [62]. The decrease in DHA observed in aged animals was mainly due to changes in PS and in a minor proportion in PE. Changes in PS composition were even more pronounced in DRMs from aged rats. A similar decrease in DHA content in PE and PS was reported for young and old rat frontal cortex and hippocampus [63]. In view of this, the loss of DHA during aging or pathological states may diminish the protective capacity in the central nervous system.

PC-PLC and PLD generate the lipid mediator DAG through the hydrolysis of PC. This sustained wave of DAG occurs without elevation of intracellular Ca^{2+} and might be related to the activation of Ca^{2+}-independent isoforms of protein kinase C (PKC) [18]. PC-PLC and PLD coexistence and their activation by oxidative stress in rat cerebral cortex synaptosomes have been already studied in our laboratory

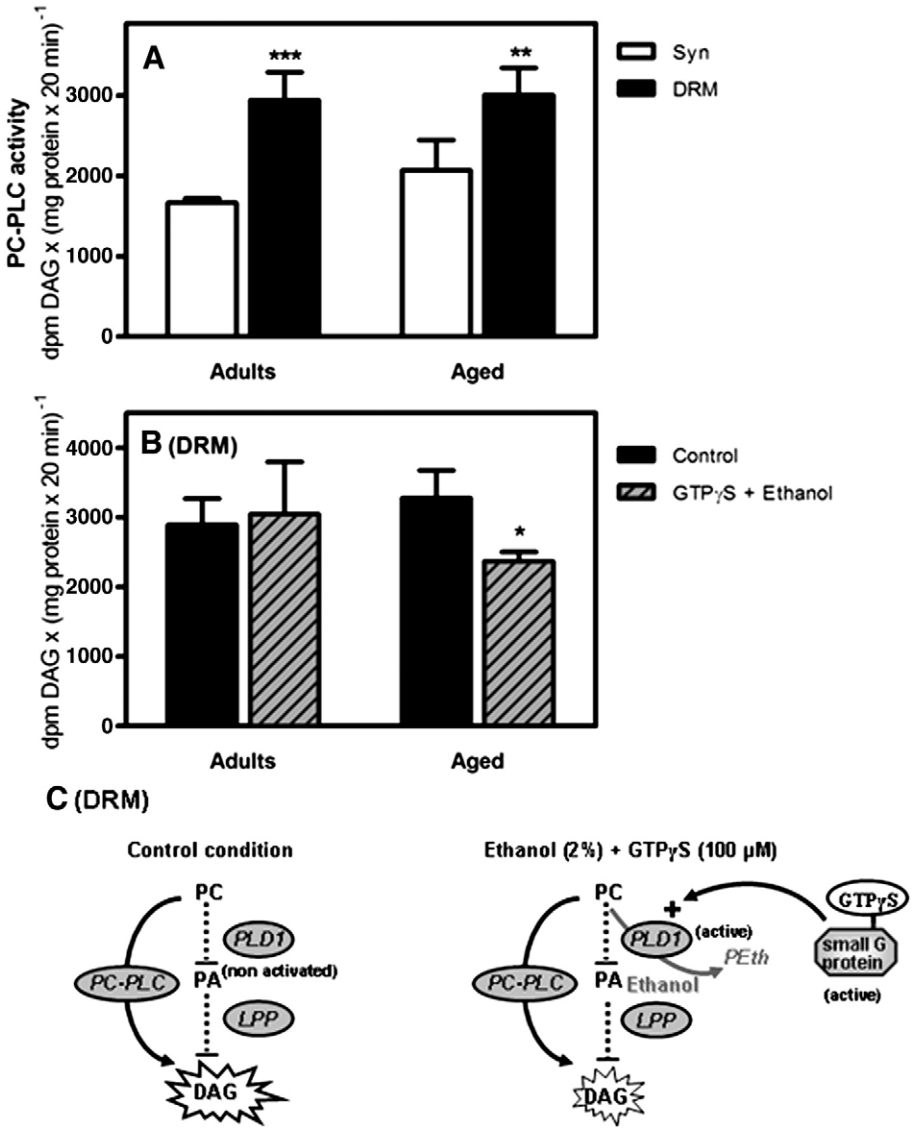

Fig. 7. (A) PC-PLC specific activity in Syn and DRMs from adult and aged rats was measured as DAG formation in the presence of 2% ethanol. The enzyme reaction was carried out as described in Fig. 6A. Results are expressed as dpm DAG × (mg protein × 20 min)$^{-1}$ and were compared between Syn and DRMs. (B) PC hydrolysis in DRMs from adult and aged rats was measured as described in Fig. 6A in the presence of vehicle (control condition) or 2% ethanol plus 100 μM GTPγS. (C) Schematic view of PLD1 activity in the DRM fraction under the different experimental conditions. Full arrows indicate active pathways while dotted lines indicate non active or inhibited pathways. Results are expressed as dpm DAG × (mg protein × 20 min)$^{-1}$ and were compared to the control condition. Data represent the mean value ± SD of at least three independent experiments using a pool of three animals on each occasion ($^{***}p<0.001$; $^{**}p<0.01$; $^{*}p<0.05$).

[20,21]. Nevertheless, the results presented in the present work constitute the first evidence of PC-PLC and PLD localization in DRM fraction from the cerebral cortex synaptic endings. A differential localization of PC-PLC and PLD isoforms in DRMs and Syn was observed; whereas PLD1 and PC-PLC were concentrated in DRMs, PLD2 was excluded from this fraction.

Using ethanol (as a transphosphatidylation reagent) and propranolol (as a LPPs inhibitor) we demonstrated that DAG generation from PC is due to PC-PLC and PLD activities in synaptic endings. It is important to notice that some of the biological events that had been attributed to PC-PLC could be due to SM synthase (SMS), an enzyme involved in SM and ceramide metabolism which transfers a phosphocholine group from PC to CM generating SM and DAG [64,65]. However, the kinetic of DAG production by SMS is significantly different from that of DAG production by PC-PLC or PLD/LPPs pathways. SMS-mediated DAG production is a much slower process and needs the addition of exogenous CM to be evidenced. Moreover, when [^{3}H-choline]-DPPC was used as a labeled substrate, no SM formation from PC was detected in synaptosomes under our experimental conditions [20].

Surprisingly, in the DRM fraction DAG formation was not decreased in the presence of ethanol indicating that no PLD activity was detected in DRMs even though PLD1 was concentrated in this fraction. It is well known that PLD1 has a very low basal activity and that it is activated by small G-proteins (ARF and Rho) and by PKCα. On the contrary, PLD2 has a higher basal activity [66,67]. Moreover, it was reported that PLD1 is inhibited by Triton X-100 [68]. PLD1 activity was only detected in DRMs from aged rats when DAG formation was measured in the presence of ethanol plus GTPγS. The activation of PLD1 in DRMs from aged rats suggests a differential regulation mechanism since that neither PLD1 localization, nor its substrate availability were altered by aging. Our results also suggest that PLD2 isoform (that harbors a high basal activity and was absent in DRMs) would be the responsible for the PLD activity observed in entire Syn under our experimental conditions. PLD1 was also located in DRM from mononuclear cells [69,70] and in caveolae from 3Y1 and COS-7 cells [13,14]. It was proposed that PLD1 localization in membrane rafts could constitute a strategy to inhibit its activity, since disruption of these domains results in relocalization and activation of the enzyme [69]. Furthermore, it was

demonstrated that PLD1 purified from rat brain directly binds to Caveolin-1 and that this union is able to inhibit PLD1 basal and PKCα-dependent activity [13]. Results obtained regarding PLD1 activity suggest that in spite of the enzyme enrichment in the DRM fraction, its localization in membrane specialized domains could be inhibiting its activity under basal conditions.

We have previously reported that PC-PLC activity was located in the synaptosomal plasma membrane fraction [20]. Here, we demonstrate that PC-PLC is enriched and active in the DRM fraction. The localization of this enzyme in membrane rafts was only previously reported in Natural Killers cells [71]. The higher substrate availability in DRMs could be also contributing to the enhanced activity of the enzyme. It is important to notice that PC-PLC activity seems not to be influenced by the lipid environment, since no differences in activity were detected between aged and adult animals in spite of the drastic changes observed in the fatty acid composition.

Even though the physiological relevance of DRMs is largely controversial their study has provided important advances in the field of signal transduction. Results presented here show a selective localization of PC-derived signaling between DRMs and synaptic endings. This work constitutes the first evidence of PC-PLC localization and activity in these specialized domains in the central nervous system. Moreover, the distinct fatty acyl composition in Syn and DRMs from aged rats could be responsible, at least in part, for the signaling impairment and neuronal dysfunction observed during aging.

Acknowledgements

This work was supported by grants from the Universidad Nacional del Sur, the Consejo Nacional de Investigaciones Científicas y Técnicas (CONICET) and the Agencia Nacional de Promoción Científica (ANPCYT) to N.M.G and G.A.S. N.M.G and G.A.S are research members of the CONICET. M.V.M is postdoctoral research fellow of the CONICET. We want to thank Dr. G.M. Oresti and Dr. N.E. Furland for their help with GLC analysis, Dr. D. Raben and Dr. H. Goldfine for kindly providing the anti-PLD2 and anti-PC-PLC antibodies and Dr. A.V. Rodriguez and Dr. G. Font de Valdez for providing the anti-Flotillin-1 antibody.

References

[1] D.A. Brown, E. London, Functions of lipid rafts in biological membranes, Annu. Rev. Cell Dev. Biol. 14 (1998) 111–136.
[2] L.J. Pike, Rafts defined: a report on the Keystone Symposium on Lipid Rafts and Cell Function, J. Lipid Res. 47 (2006) 1597–1598.
[3] K. Simons, D. Toomre, Lipid rafts and signal transduction, Nat. Rev. Mol. Cell Biol. 1 (2000) 31–39.
[4] J.B. Helms, C. Zurzolo, Lipids as targeting signals: lipid rafts and intracellular trafficking, Traffic 5 (2004) 247–254.
[5] P. Lajoie, I.R. Nabi, Regulation of raft-dependent endocytosis, J. Cell Mol. Med. 11 (2007) 644–653.
[6] D.A. Brown, J.K. Rose, Sorting of GPI-anchored proteins to glycolipid-enriched membrane subdomains during transport to the apical cell surface, Cell 68 (1992) 533–544.
[7] D.A. Brown, E. London, Structure and function of sphingolipid- and cholesterol-rich membrane rafts, J. Biol. Chem. 275 (2000) 17221–17224.
[8] S. Maekawa, S. Iino, S. Miyata, Molecular characterization of the detergent-insoluble cholesterol-rich membrane microdomain (raft) of the central nervous system, Biochim. Biophys. Acta 1610 (2003) 261–270.
[9] D. Lichtenberg, F.M. Goni, H. Heerklotz, Detergent-resistant membranes should not be identified with membrane rafts, Trends Biochem. Sci. 30 (2005) 430–436.
[10] M.G. Waugh, J.J. Hsuan, Preparation of membrane rafts, Methods Mol. Biol. 462 (2009) 403–414.
[11] C.J. Clarke, S. Forman, J. Pritchett, V. Ohanian, J. Ohanian, Phospholipase C-delta1 modulates sustained contraction of rat mesenteric small arteries in response to noradrenaline, but not endothelin-1, Am. J. Physiol Heart Circ. Physiol. 295 (2008) H826–H834.
[12] M. Czarny, Y. Lavie, G. Fiucci, M. Liscovitch, Localization of phospholipase D in detergent-insoluble, caveolin-rich membrane domains. Modulation by caveolin-1 expression and caveolin-182-101, J. Biol. Chem. 274 (1999) 2717–2724.
[13] J.H. Kim, J.M. Han, S. Lee, Y. Kim, T.G. Lee, J.B. Park, S.D. Lee, P.G. Suh, S.H. Ryu, Phospholipase D1 in caveolae: regulation by protein kinase Calpha and caveolin-1, Biochemistry 38 (1999) 3763–3769.
[14] Y. Kim, J.M. Han, B.R. Han, K.A. Lee, J.H. Kim, B.D. Lee, I.H. Jang, P.G. Suh, S.H. Ryu, Phospholipase D1 is phosphorylated and activated by protein kinase C in caveolin-enriched microdomains within the plasma membrane, J. Biol. Chem. 275 (2000) 13621–13627.
[15] E. Szymanska, M. Korzeniowski, P. Raynal, A. Sobota, K. Kwiatkowska, Contribution of PIP-5 kinase Ialpha to raft-based FcgammaRIIA signaling, Exp. Cell Res. 315 (2009) 981–995.
[16] M. Yamaga, K. Kawai, M. Kiyota, Y. Homma, H. Yagisawa, Recruitment and activation of phospholipase C (PLC)-delta1 in lipid rafts by muscarinic stimulation of PC12 cells: contribution of p122RhoGAP/DLC1, a tumor-suppressing PLCdelta1 binding protein, Adv. Enzyme Regul. 48 (2008) 41–54.
[17] M.M. Billah, J.C. Anthes, The regulation and cellular functions of phosphatidylcholine hydrolysis, Biochem. J. 269 (1990) 281–291.
[18] Z. Cui, M. Houweling, Phosphatidylcholine and cell death, Biochim. Biophys. Acta 1585 (2002) 87–96.
[19] J.H. Exton, Phosphatidylcholine breakdown and signal transduction, Biochim. Biophys. Acta 1212 (1994) 26–42.
[20] M.V. Mateos, R.M. Uranga, G.A. Salvador, N.M. Giusto, Coexistence of phosphatidylcholine-specific phospholipase C and phospholipase D activities in rat cerebral cortex synaptosomes, Lipids 41 (2006) 273–280.
[21] M.V. Mateos, R.M. Uranga, G.A. Salvador, N.M. Giusto, Activation of phosphatidylcholine signalling during oxidative stress in synaptic endings, Neurochem. Int. 53 (2008) 199–206.
[22] G.A. Salvador, S.J. Pasquare, M.G. Ilincheta de Boschero, N.M. Giusto, Differential modulation of phospholipase D and phosphatidate phosphohydrolase during aging in rat cerebral cortex synaptosomes, Exp. Gerontol. 37 (2002) 543–552.
[23] G.A. Salvador, M.G. Ilincheta, S.J. de Boschero, N.M. Giusto Pasquare, Phosphatidic acid and diacylglycerol generation is regulated by insulin in cerebral cortex synaptosomes from adult and aged rats, J. Neurosci. Res. 81 (2005) 244–252.
[24] C.W. Cotman, Isolation of synaptosomal and synaptic plasma membrane fractions, Methods Enzymol. 31 (1974) 445–452.
[25] O.H. Lowry, N.J. Rosebrough, A.L. Farr, R.J. Randall, Protein measurement with the Folin phenol reagent, J. Biol. Chem. 193 (1951) 265–275.
[26] M. Molander-Melin, K. Blennow, N. Bogdanovic, B. Dellheden, J.E. Mansson, P. Fredman, Structural membrane alterations in Alzheimer brains found to be associated with regional disease development; increased density of gangliosides GM1 and GM2 and loss of cholesterol in detergent-resistant membrane domains, J. Neurochem. 92 (2005) 171–182.
[27] G.A. Salvador, N.M. Giusto, Characterization of phospholipase D activity in bovine photoreceptor membranes, Lipids 33 (1998) 853–860.
[28] J. Folch, M. Lees, G.H. Sloane Stanley, A simple method for the isolation and purification of total lipides from animal tissues, J. Biol. Chem. 226 (1957) 497–509.
[29] E.G. Bligh, W.J. Dyer, A rapid method of total lipid extraction and purification, Can. J. Biochem. Physiol. 37 (1959) 911–917.
[30] G. Rouser, S. Fkeischer, A. Yamamoto, Two dimensional then layer chromatographic separation of polar lipids and determination of phospholipids by phosphorus analysis of spots, Lipids 5 (1970) 494–496.
[31] N.E. Furland, E.N. Maldonado, P.A. Aresti, M.I. Aveldano, Changes in lipids containing long- and very long-chain polyunsaturated fatty acids in cryptorchid rat testes, Biol. Reprod. 77 (2007) 181–188.
[32] U.K. Laemmli, Cleavage of structural proteins during the assembly of the head of bacteriophage T4, Nature 227 (1970) 680–685.
[33] P.E. Bickel, P.E. Scherer, J.E. Schnitzer, P. Oh, M.P. Lisanti, H.F. Lodish, Flotillin and epidermal surface antigen define a new family of caveolae-associated integral membrane proteins, J. Biol. Chem. 272 (1997) 13793–13802.
[34] A.M. Hartmann, P. Blaesse, T. Kranz, M. Wenz, J. Schindler, K. Kaila, E. Friauf, H.G. Nothwang, Opposite effect of membrane raft perturbation on transport activity of KCC2 and NKCC1, J. Neurochem. 111 (2009) 321–331.
[35] C.A. Stuermer, The reggie/flotillin connection to growth, Trends Cell Biol. (2009).
[36] M.A. Clark, R.G. Shorr, J.S. Bomalaski, Antibodies prepared to Bacillus cereus phospholipase C crossreact with a phosphatidylcholine preferring phospholipase C in mammalian cells, Biochem. Biophys. Res. Commun. 140 (1986) 114–119.
[37] C. Ramoni, F. Spadaro, M. Menegon, F. Podo, Cellular localization and functional role of phosphatidylcholine-specific phospholipase C in NK cells, J. Immunol. 167 (2001) 2642–2650.
[38] F. Spadaro, S. Cecchetti, M. Sanchez, C.M. Ausiello, F. Podo, C. Ramoni, Expression and role of phosphatidylcholine-specific phospholipase C in human NK and T lymphocyte subsets, Eur. J. Immunol. 36 (2006) 3277–3287.
[39] C.E. Naylor, J.T. Eaton, A. Howells, N. Justin, D.S. Moss, R.W. Titball, A.K. Basak, Structure of the key toxin in gas gangrene, Nat. Struct. Biol. 5 (1998) 738–746.
[40] Y. Nozawa, Roles of phospholipase D in apoptosis and pro-survival, Biochim. Biophys. Acta 1585 (2002) 77–86.
[41] M. Kobayashi, J.N. Kanfer, Phosphatidylethanol formation via transphosphatidylation by rat brain synaptosomal phospholipase D, J. Neurochem. 48 (1987) 1597–1603.
[42] A.P. Albert, A.S. Piper, W.A. Large, Role of phospholipase D and diacylglycerol in activating constitutive TRPC-like cation channels in rabbit ear artery myocytes, J. Physiol. 566 (2005) 769–780.
[43] K.E. Meier, K.C. Gause, A.E. Wisehart-Johnson, A.C. Gore, E.L. Finley, L.G. Jones, C.D. Bradshaw, A.F. McNair, K.M. Ella, Effects of propranolol on phosphatidate phosphohydrolase and mitogen-activated protein kinase activities in A7r5 vascular smooth muscle cells, Cell Signal. 10 (1998) 415–426.
[44] H.A. Brown, S. Gutowski, C.R. Moomaw, C. Slaughter, P.C. Sternweis, ADP-ribosylation factor, a small GTP-dependent regulatory protein, stimulates phospholipase D activity, Cell 75 (1993) 1137–1144.
[45] J.H. Exton, Regulation of phospholipase D, Biochim. Biophys. Acta 1439 (1999) 121–133.

[46] A.W. Cohen, R. Hnasko, W. Schubert, M.P. Lisanti, Role of caveolae and caveolins in health and disease, Physiol. Rev. 84 (2004) 1341–1379.
[47] D.P. de, T. Medts, S. Carpentier, L. D'Auria, S.P. Van Der, A. Platek, M. Mettlen, A. Caplanusi, M.F. van den Hove, D. Tyteca, P.J. Courtoy, Differential subcellular membrane recruitment of Src may specify its downstream signalling, Exp. Cell Res. 314 (2008) 1465–1479.
[48] H. Lee, D.S. Park, X.B. Wang, P.E. Scherer, P.E. Schwartz, M.P. Lisanti, Src-induced phosphorylation of caveolin-2 on tyrosine 19. Phospho-caveolin-2 (Tyr(P)19) is localized near focal adhesions, remains associated with lipid rafts/caveolae, but no longer forms a high molecular mass hetero-oligomer with caveolin-1, J. Biol. Chem. 277 (2002) 34556–34567.
[49] R.E. Martin, M.H. Elliott, R.S. Brush, R.E. Anderson, Detailed characterization of the lipid composition of detergent-resistant membranes from photoreceptor rod outer segment membranes, Invest. Ophthalmol. Vis. Sci. 46 (2005) 1147–1154.
[50] S. Maekawa, C. Sato, K. Kitajima, N. Funatsu, H. Kumanogoh, Y. Sokawa, Cholesterol-dependent localization of NAP-22 on a neuronal membrane microdomain (raft), J. Biol. Chem. 274 (1999) 21369–21374.
[51] M.D. Resh, Fatty acylation of proteins: new insights into membrane targeting of myristoylated and palmitoylated proteins, Biochim. Biophys. Acta 1451 (1999) 1–16.
[52] N.M. Giusto, G.A. Salvador, P.I. Castagnet, S.J. Pasquare, M.G. Ilincheta de Boschero, Age-associated changes in central nervous system glycerolipid composition and metabolism, Neurochem. Res. 27 (2002) 1513–1523.
[53] G.Y. Sun, T. Samorajski, Age changes in the lipid composition of whole homogenates and isolated myelin fractions of mouse brain, J. Gerontol. 27 (1972) 10–17.
[54] G.Y. Sun, T. Samorajski, Age differences in the acyl group composition of phosphoglycerides in myelin isolated from the brain of the rhesus monkey, Biochim. Biophys. Acta 316 (1973) 19–27.
[55] G.H. Lopez, M.G. Ilincheta, P.I. de Boschero, N.M. Giusto Castagnet, Age-associated changes in the content and fatty acid composition of brain glycerophospholipids, Comp. Biochem. Physiol. B Biochem. Mol. Biol. 112 (1995) 331–343.
[56] N.M. Giusto, M.E. Roque, M.G. Ilincheta de Boschero, Effects of aging on the content, composition and synthesis of sphingomyelin in the central nervous system, Lipids 27 (1992) 835–839.
[57] H.Y. Kim, J. Hamilton, Accumulation of docosahexaenoic acid in phosphatidylserine is selectively inhibited by chronic ethanol exposure in C-6 glioma cells, Lipids 35 (2000) 187–195.
[58] H.Y. Kim, Novel metabolism of docosahexaenoic acid in neural cells, J. Biol. Chem. 282 (2007) 18661–18665.
[59] N. Salem Jr., B. Litman, H.Y. Kim, K. Gawrisch, Mechanisms of action of docosahexaenoic acid in the nervous system, Lipids 36 (2001) 945–959.
[60] M. Martinez, Severe deficiency of docosahexaenoic acid in peroxisomal disorders: a defect of delta 4 desaturation? Neurology 40 (1990) 1292–1298.
[61] M. Soderberg, C. Edlund, K. Kristensson, G. Dallner, Fatty acid composition of brain phospholipids in aging and in Alzheimer's disease, Lipids 26 (1991) 421–425.
[62] H.Y. Kim, Biochemical and biological functions of docosahexaenoic acid in the nervous system: modulation by ethanol, Chem. Phys. Lipids 153 (2008) 34–46.
[63] S. Favrelere, S. Stadelmann-Ingrand, F. Huguet, J.D. De, A. Piriou, C. Tallineau, G. Durand, Age-related changes in ethanolamine glycerophospholipid fatty acid levels in rat frontal cortex and hippocampus, Neurobiol. Aging 21 (2000) 653–660.
[64] C. Luberto, Y.A. Hannun, Sphingomyelin synthase, a potential regulator of intracellular levels of ceramide and diacylglycerol during SV40 transformation. Does sphingomyelin synthase account for the putative phosphatidylcholine-specific phospholipase C? J. Biol. Chem. 273 (1998) 14550–14559.
[65] C. Luberto, D.S. Yoo, H.S. Suidan, G.M. Bartoli, Y.A. Hannun, Differential effects of sphingomyelin hydrolysis and resynthesis on the activation of NF-kappa B in normal and SV40-transformed human fibroblasts, J. Biol. Chem. 275 (2000) 14760–14766.
[66] J.H. Exton, Regulation of phospholipase D, FEBS Lett. 531 (2002) 58–61.
[67] J. Klein, Functions and pathophysiological roles of phospholipase D in the brain, J. Neurochem. 94 (2005) 1473–1487.
[68] I.N. Singh, L.M. Stromberg, S.G. Bourgoin, V.A. Sciorra, A.J. Morris, D.N. Brindley, Ceramide inhibition of mammalian phospholipase D1 and D2 activities is antagonized by phosphatidylinositol 4, 5-bisphosphate, Biochemistry 40 (2001) 11227–11233.
[69] O. Diaz, A. Berquand, M. Dubois, A.S. Di, C. Sette, S. Bourgoin, M. Lagarde, G. Nemoz, A.F. Prigent, The mechanism of docosahexaenoic acid-induced phospholipase D activation in human lymphocytes involves exclusion of the enzyme from lipid rafts, J. Biol. Chem. 277 (2002) 39368–39378.
[70] O. Diaz, S. Mebarek-Azzam, A. Benzaria, M. Dubois, M. Lagarde, G. Nemoz, A.F. Prigent, Disruption of lipid rafts stimulates phospholipase d activity in human lymphocytes: implication in the regulation of immune function, J. Immunol. 175 (2005) 8077–8086.
[71] S. Cecchetti, F. Spadaro, L. Lugini, F. Podo, C. Ramoni, Functional role of phosphatidylcholine-specific phospholipase C in regulating CD16 membrane expression in natural killer cells, Eur. J. Immunol. 37 (2007) 2912–2922.

Glossary

AA: arachidonic acid
CC: cerebral cortex
CM: ceramida
Chol: cholesterol
CTB-HRP: cholera toxin subunit B-HRP-conjugated
DAG: diacylglycerol
DHA: docosahexaenoic acid
DPPC: dipalmitoylphosphatidylcholine
DRMs: detergent-resistant membranes
DTT: dithiothreitol
EDTA: ethylenediaminetetraacetic acid
FAME: fatty acid methyl ester
FFA: free fatty acid
GLC: gas–liquid chromatography
GTPγS: Guanosine 5′-[*gamma*-thio]triphosphate
HEPES: 4-(2-hydroxyethyl)-1-piperazine ethanesulfonic acid
HRP: horseradish peroxidise
lipid P: lipid phosphorus
LPPs: lipid phosphate phosphatases
MAG: monoacylglycerol
NLs: neutral lipids
PA: phosphatidic acid
PAP: phosphatidic acid phosphohydrolase
PC: phosphatidylcholine
PC-PLC: phosphatidylcholine-specific-phospholipase C
PE: phosphatidylethanolamine
PI: phosphatidylinositol
PIP_2: phosphatidylinositol bisphosphate
PKC: protein kinase C
PLD: phospholipase D
PLs: phospholipids
PMSF: phenylmethylsulfonilfluoride
PS: phosphatidylserine
PUFA: polyunsaturated fatty acids
PVDF: polyvinylidene fluoride
SDS: sodium dodecyl sulfate
SDS-PAGE: sodium dodecyl sulfate-polyacrylamide gel electrophoresis
SM: sphingomyelin
SMS: sphingomyelin synthase
Syn: synaptosomes
TBM: tris buffer medium
TLC: thin-layer chromatography
UI: unsaturation index
WB: Western blot